Sohag Journal of Sciences
An International Journal

Geomagnetic characterization of a basaltic intrusion and its tectonic implications, Eastern Desert, Egypt

Abdelbaset M. Abudeif*, Saad E. Saad, Mohammed A. Mohammed
Geology Department, Faculty of Science, Sohag University, Sohag, 82524, Egypt

Received: 2 July 2022, Revised: 18 July 2022, Accepted: 18 July 2022.
Published online: 1sept. 2022

Abstract: The purpose of this study is to define the geographic area of an estimated depth to an Eastern desert intrusion near wadi Qena. The study also clarified the many stages of deformations connected to this intrusion. Aeromagnetic data was employed using the goal of this investigation for this purpose. Along with the underlying structure, these intrusions' depths and magnetic susceptibilities were evaluated. To get RTP magnetic data with anomalies concentrated on the subsurface causal bodies, the magnetic data was reduced to the North Pole. Various filtering methods were used. The power spectrum approach was used to determine the distance to the causative bodies. The maps reveal significant magnetic anomalies caused by basaltic intrusion inside sedimentary strata with a general NNW-SSE trend and very probable multi-phase intrusion activity. Calcite crystals were seen in a few of the measured joints. Various techniques are used to determine the major depth to the causative bodies.

Keywords: Aeromagnetic –Eastern Desert- Filtering- Subsurface structure

1 Introduction

Magnetic anomalies are caused by differences in the physical characteristics of rocks (magnetization). This technique still allows for the study of magnetic fluctuations throughout the Earth's crust, but it is more susceptible to the influence of rocks close to the surface than those buried at considerable depths.

In addition to the information offered by the magnetic field on the map, filtering the magnetic data allows one to learn more about the structure of the basement and the underlying sedimentary successions.

More information on the layout of the main events that affect the area can be obtained by using recent filtering techniques, such as the multi-scale analysis of the geological contacts based on the coupling of horizontal derivative and downward continuation (Blakely 1996; Blakely and Simpson 1986; Chennouf et al. 2007; Cordell and Grauch 1982; Cordell and Grauch 1985; Everaerts and Mansy 2001; Khattach et al. 2006). This method can be used to estimate the length, dip, and depth of these events.

The study is located in the Eastern Desert, Egypt west of Wadi Qena by a distance of about 40 km. It is bounded by latitudes 26º 45` 00" N and 26º 52` 50"N and longitudes 32º 15` 00"E and 32º 30` 00"E (Fig.1), It is distinguished by the variety in topography, geomorphology, rock units, geological structures, and the drainage patterns. The area is accessible either from Sohag or from Safaga by the Sohag-Red Sea Road.

The present study aims essentially to evaluate the influence of the intrusion of basaltic intrusions within the sedimentary cover.

Aeromagnetic data was processed and interpreted along group of profiles. A total magnetic intensity map was created by correcting the measured magnetic field (Fig.4a). To obtain an RTP map, this map was scaled down to the northern magnetic pole (Fig.4b).

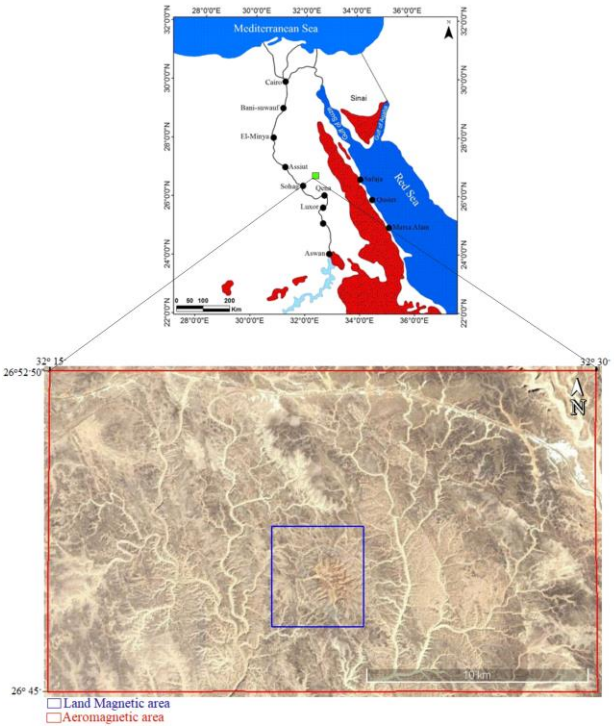

Fig. 1. Location map of the research region, the blue color indicates the area of land magnetic survey included within a large area of aeromagnetic data with the red color.

* Corresponding author E-mail: a.abudeif@science.sohag.edu.eg

Geologic setting

The Lower Eocene carbonate plateau, which covers the research region, is divided into several valleys (Wadis) of Resent formations that run roughly in a NW-SE direction (Fig.2 and 3). Some of these Wadis flow parallel to the Nile Valley and in the general direction of the topographic slope, while other streams flow in the opposite direction of the formations' dips and their following streams (Abdel Moneim 1988; Ismaiel and Badry 2012). The exposed Lower Eocene carbonate sequence was subdivided Lithostratigraphically by Keheila and El-Ayyat (1990) into two rock units: 1- The Thebes Formation and 2- Drunka Formation. Interfingering and time counterpart are the relationships between the two units (Shaaban 2004).

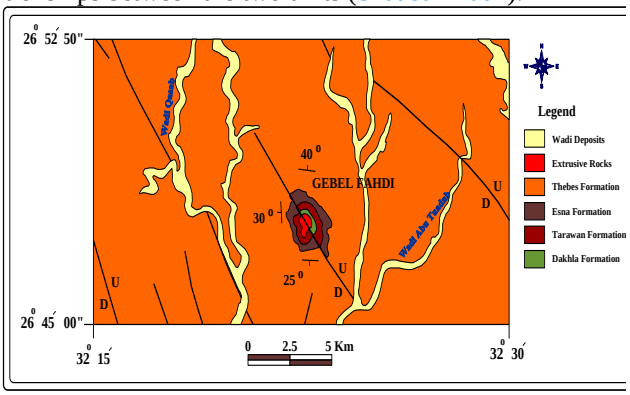

Fig. 2. Detailed geology map of the research area. (CONOCO. 1987 and EGSMA 1983 & 2006).

Fig. 3. different types of limestone rocks exposed along the study area after Ismaiel and Badry (2012) **.**

2. Material and methods

The following geological and geophysical data, together with the available software, were used to complete the current study:

- Total aeromagnetic intensity anomaly map. Geosoft Oasis Montaj Software V.8.4, 2015 was used to process and analyze the data.
- The surface geology and structures of Egypt were depicted on the geological map of Egypt (scale 1:500.000) issued by EGPC and CONOCO (1987).
- The available software as Surfer 10.0 (2011).
- The available published geological and geophysical studies of the area.

2.1. Aeromagnetic data processing

Digitizing can be defined as transformation of the data from the analogue form (map sheets) to digital form. The contoured aeromagnetic is converted into a digital status as the initial step in the analysis procedure of the geophysical data. This step is applied by enlarging the original maps size which have scale 1:500,000 to reach the scale 1: 100,000 for the aeromagnetic data. This means that the dimension of the grid node in the aeromagnetic map was (1x1 cm). Then relating to the coordinates, the values were picked to obtain the (Z) value with that regular distance. The recorded (Z) value is the value of the contour line of magnetic intensity at certain (X, Y) point. The study area is sampled as a set of rows and columns, it is composed of 203 columns and 112 rows, and this means that the Z values reached 22,736 records for the aeromagnetic map. This huge amount of the obtained values was ordered and input on a computer file as (X, Y, Z) in an excel data sheet and treated by the Surfer v.10 (2011) or any of gridding software. The interpolation of data with asymmetrical spacing into a matrix is known as gridding. Gridding can be done using a variety of techniques, such as kriging and various weighted averages, such as minimal curvature gridding. To complete this process in the current investigation, the digitizing magnetic data were applied to the file GRID utility provided by the Geosoft Oasis Montaj V.8.4 (2015).

In this work, the different resulted maps derived from the applied software (Geosoft Oasis Montaj V.8.4 (2015) by analysis the input gridded (X, Y, Z) data into the needed option by Fast Fourier Transformation. After that the grid utility process made to prepare the data into the final step, which is converting the Geosoft (X, Y, and Z) into output (X, Y, Z) with extension data.

Finally, the obtained gridded data sets can be contoured and prepared to display but there is another advanced technique used for better data displaying and more representative known as shaded color relief maps, this technique used for all maps on this study, where the data plotted in a color range with 3D shade. Fig (4a) shows the resultant total magnetic intensity aeromagnetic anomaly map.

2.2. Reduction to the pole (RTP) method

The geomagnetic vector at the observation spots and the magnetization vector inside the concealed causal body in the subsurface determine the amount and shape of the magnetic deviations produced on the total intensity map. A single positive magnetic anomaly at the magnetic poles or a single negative magnetic anomaly at the equator can both be caused by the same causal item at different magnetic latitudes. Because of the indicated magnetization vector's direction, it can be claimed that the observed total intensity aeromagnetic map contains more or less deceptive anomalies. This is due to the fact that, at low or moderate geomagnetic field inclination angles, the peak of the highest

curvature generated by the body relocated away from over the center of the magnetized bodies, making it challenging to pinpoint the precise location of these bodies. To evaluate a hypothetical anomaly of the observed kind where the causal body can be directed as to be seen with respect to the magnetic north pole on the total intensity map is therefore advised for a good accuracy of interpretation of the magnetic maps. Consequently, the magnetization vector will be more or less vertical by applying the reduction to magnetic pole techniques (Baranov, 1957). The value of normal (IGRF-15/4/2014) geomagnetic field for the study area is (F) is 42088.5 gamma, declination (D) is 3.85, inclination (I) is 39.19. Using Geosoft software, the total magnetic intensity was reduced to the north magnetic pole (RTP), and the result was shown in Figure 4b.

2.3. Magnetic Filtering

The following filtering techniques were applied in this study using Geosoft Oasis Montag Software V.8.4:

a) Low pass filter

Low pass filter also applied on RTP map by Geosoft Oasis Montaj software version .8.4 (2015) with parameters of degree of filter function is 8, the central wave number is 0.005 (cycle/ground unit) to remove the influences of the local magnetic field and its noise for producing the regional anomaly map (Hesham et al, 2016 and Khalil et al, 2016). Figure 5a displays the final map.

b) High pass filter (Residual)

To improve the signal characteristics of the existing data, the RTP magnetic map was filtered in the frequency domain using a high pass filter to produce a residual map with parameters of degree of filter function of 8 and center wave number of 0.15 (cycle/ground unit) (Cooper, 1997). The high pass filter is used to bring details in the map with the risk of enhancing noise. The resulted map is shown in Figure 5b.

2.4. Structural tectonic trend analysis

By comparing the structures inferred from surface studies with those inferred from geophysical data, the tectonic interpretation of the studied region is constructed. The subsurface structural lines were traced according to Gay's principles (1972), from magnetic maps (the total magnetic intensity (TMI) (Fig.4a), reduction-to-pole (RTP), (Fig.4b), low pass filter (Fig.5a), high pass filter (Fig.5b to follow the subsurface structures at different planes).

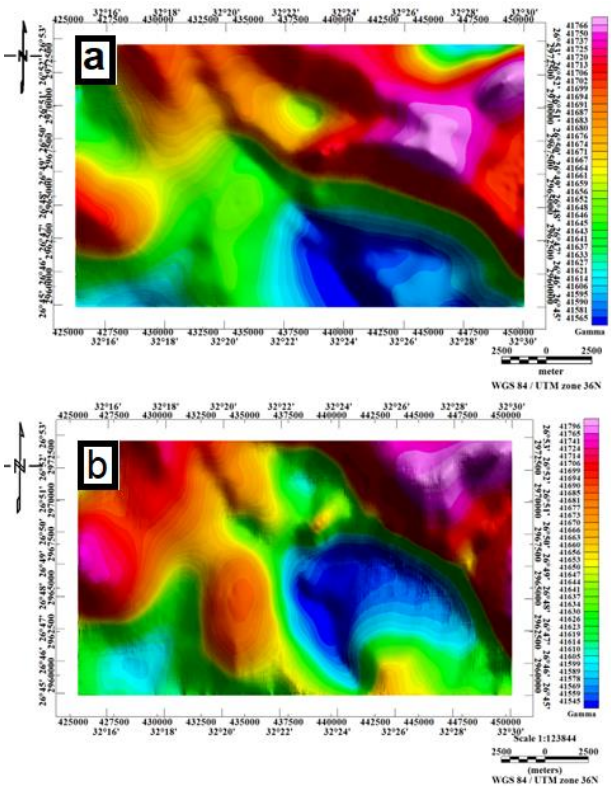

Fig.4. The maps in (a) and (b) show the study area's total magnetic field intensity and reduced to the pole (RTP) maps, respectively.

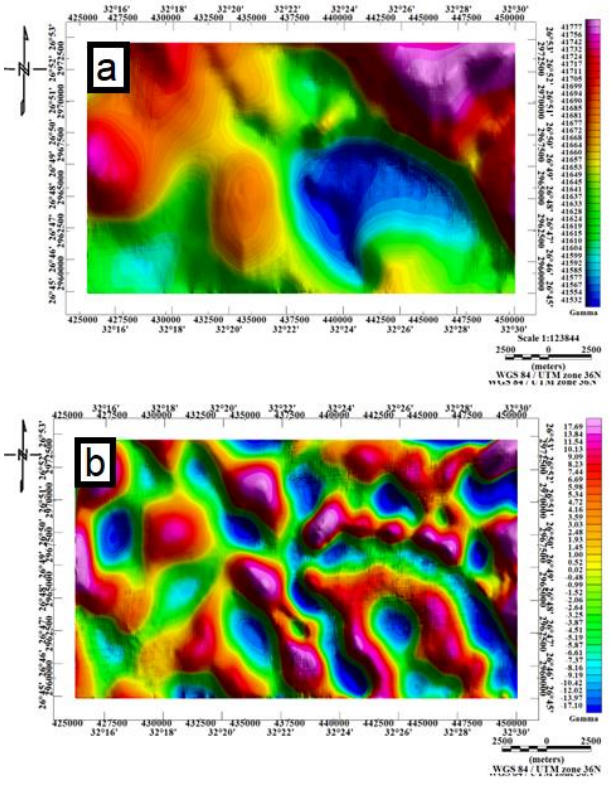

Fig. 5. (a) is a Shaded color relief map of the Low Pass (regional) and **(**b) is a Shaded color relief map of the high Pass (residual) of the studied area.

2.5. Quantitative interpretation of magnetic data

Utilizing Geosoft Oasis Montaj V 8.4 (2015) software, the total magnetic intensity reduced to the pole (RTP) map is quantitatively interpreted.

The applied methods of quantitative analysis of magnetic data in this study include:

- Determination of the basement depth using different methods, which were applied to profiles crossing the anomalies and gridded data sets of the RTP magnetic field map.
- Defining the source location using three-dimensional analytical signal.

3. Results & Discussion

The main trends of the anomalies, the depth to the causative bodies, the tectonic history, the subsurface structures affecting both the basement rock and the sedimentary cover, as well as the topography of the basement rock, were all described using the qualitative and quantitative interpretation of the magnetic data.

3.1. Results of qualitative analysis of the magnetic data.

3.1.1.RTP

The interpretation results of this study for RTP (Fig.4b) reveal that:

1. The anomalies' spatial locations are depicted on the map with a slight spatial variation from the total magnetic intensity map's original data.
2. The mean trends are oriented N -S with small tends NW-SE and E-W.
3. The reduced to pole map shows anomalies with magnitude range from 41920 gamma in the northeastern part to 41516 gammas in the middle to the southeastern part of the area with a mean value of about 41654. The most peaks shown in the northeastern and the west, and finally at the middle part.
4. On this map, the relative positions of both high and low magnetic anomalies don't move all that much, the anomalies have higher resolution than the total intensity map. they are shifted slightly to the north east side of the map.
5. The gradient of magnetic anomalies increased around the main anomaly zones, that located to the northeastern, middle, and northwestern portions of the study region. this can refer to shallow depth to basement rocks or high magnetized bodies.
6. In the northeastern and northwestern of the study region, there is a collected zone of high anomalies, this detect that even the causative body may be near to surface, or contain high number of magnetic substances along an elongated structure.
7. There is also a group of magnetic lows in the middle and southwestern parts of the study area, these parts may reflect high thickness of sediments, and high depth to basement.

3.1.2. Low Pass (LP) (regional) map

The inspection of the obtained low pass (regional) map (Fig.5a) revealed that:

1. The positive anomalies have elongated shape and it take NW-SE direction with high magnitude at the northwestern and southern parts and circular shape at the northeastern part which have short wavelength and higher frequencies which mean the causative bodies buried at shallow depths, it represents the uplifted parts of the study area, and it may be caused by intrusive body with a huge extension.
2. The negative anomalies have circular and oval shapes at the middle and southwestern parts which have long wavelength and lower frequencies which mean the causative bodies buried at deep depths, it represents subsidence parts of the study area and it have a thick sedimentary cover.
3. The Low Pass filter thus gave an impression of the uplifted and subsidence parts at the study area. Consequently, more potentiality for basement rock at the study area.

3.1.3. High Pass (HP) (residual) map

The inspection of the obtained high pass (residual) map (Fig.5b) reveals that:

1. Positive and negative anomalies with higher resolution than those on the RTP map are clearly visible in the residual magnetic component with high pass characteristics.
2. These anomalies have elongated shape at the southeastern and middle parts and oval shape at the northwestern and northern parts and irregular shapes in the rest of the map area which have short wavelength and higher frequencies.
3. These anomalies, which exhibit local change, may be the result of differences in the sources' depths and composition. In the research area, the major tendencies N-S, NW-SE, NE-SW, and E-W orientations are discernible as a near-surface structure.

3.2. Results of Structural tectonic trend analysis

Structural tectonic trend analysis was discussed for the subsurface magnetic maps. The structural analysis of fault trends from rose (azimuth frequency) diagrams indicated that the most predominant fault trends are N 40°-55° E, N 60° –75° E, and N 30°-45° W trends, with less abundance of NNE-SSW and N-S. Most of the strata are dipping outward due to the injection of the tertiary basalt. The intrusion is forming in different phases where the dipping of the strata is varying from 40^{o} to 25^{o}. Subsurface

Structural Trend Analysis was done from tracing the lineaments from the aeromagnetic map. For the aeromagnetic maps, the maps of TMI, RTP, HP, LP are traced and analyzed to achieve an idea about tectonic trends affecting subsurface. Rose (azimuth frequency) diagrams are used to quantitatively evaluate and visualize lineament systems (**Figs. 6-8**). Carful inspection of the different plots reveal that:

- Most dominant trend in subsurface is the N-S, this trend is representing the first most common trend in the study area. It was recorded more or less in all magnetic maps. It is referred to as the Nubian trend, was passed down through the basement rocks of Egypt, and is viewed as a continuation of the Mozambique belt. This tendency is taken into account as a deformation strain as a result of a significant stress acting on the research region in a direction opposite to this trend (E-W).
- The second trend is the NW–SE trend. It related to Eritrean and Gulf of Suez fault trend. It results due to NE-SW stress affecting the area.
- The third concluded trend is E-W (Tethyian trend). This trend is represented in the most magnetic maps. The most significant underlying trend, which is the E-W trend, has relatively little extension on the surface map. It might be because the majority of E-W lineaments connect basement rock units with various magnetic susceptibilities. It forms as a result of N-S tension in the research region.
- The fourth deduced trend is the NE – SW (Aqaba trend). The NE-SW trend was the fourth determined trend (Aqaba trend). This trend is the most significant surface structural trend in the examined area, although it is extremely uncommon as a subsurface structural trend. It fits with the Qattara movement.

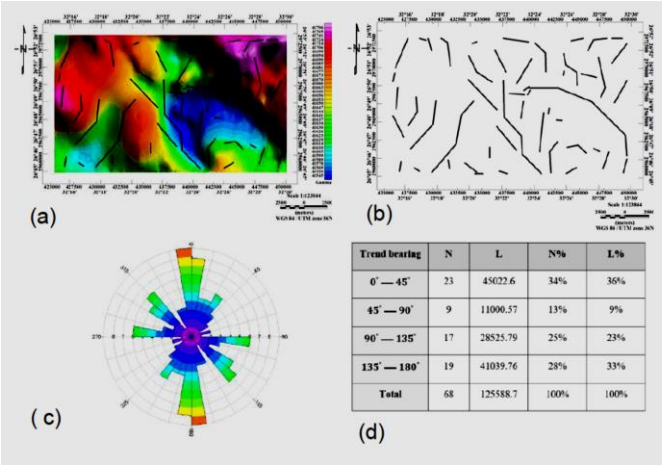

Trend bearing	N	L	N%	L%
0° — 45°	23	45022.6	34%	36%
45° — 90°	9	11000.57	13%	9%
90° — 135°	17	28525.79	25%	23%
135° — 180°	19	41039.76	28%	33%
Total	68	125588.7	100%	100%

Fig.6. Magnetic structure lines drawn from the reduced to the pole (RTP), where: (a) represents these lineaments superimposed on the original RTP map, (b) is the magnetic structural lineaments only, (c) is the rose diagram of these lineaments and (d) is the table of azimuth frequency distribution of these lineaments.

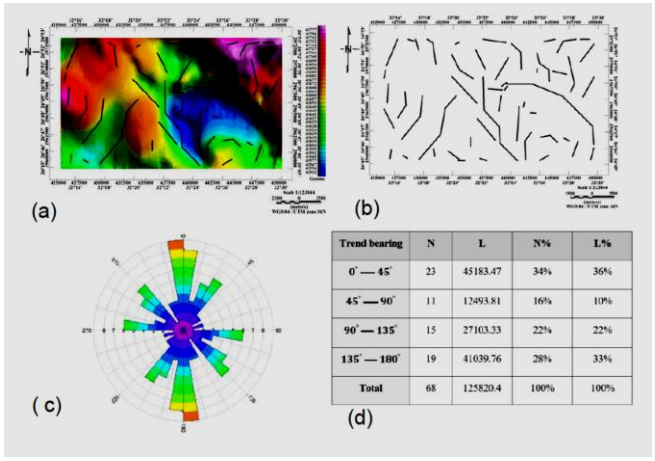

Trend bearing	N	L	N%	L%
0° — 45°	23	45183.47	34%	36%
45° — 90°	11	12493.81	16%	10%
90° — 135°	15	27103.33	22%	22%
135° — 180°	19	41039.76	28%	33%
Total	68	125820.4	100%	100%

Fig.7. Magnetic structural lineaments traced from Low pass filtering (Regional) map with cut of value 50 wave number km, where: (a) represents these lineaments superimposed on the original map, (b) is the magnetic structural lineaments only, (c) is the rose diagram of these lineaments and (d) is the table of azimuth frequency distribution of these lineaments.

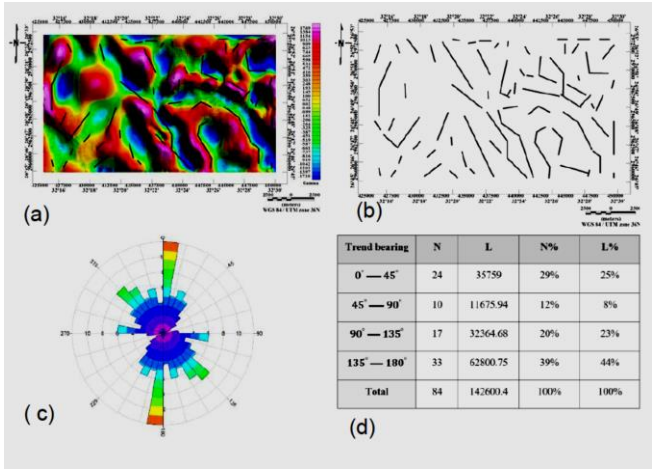

Trend bearing	N	L	N%	L%
0° — 45°	24	35759	29%	25%
45° — 90°	10	11675.94	12%	8%
90° — 135°	17	32364.68	20%	23%
135° — 180°	33	62800.75	39%	44%
Total	84	142600.4	100%	100%

Fig.8. Magnetic structural lineaments traced from high pass filling (residuals) of RTP magnetic anomaly map, where: (a) represents these lineaments superimposed on the original map, (b) is the magnetic structural lineaments only, (c) is the rose diagram of these lineaments and (d) is the table of azimuth frequency distribution of these lineaments.

3.3. Basement Depth Estimation

3.3.1. Two-Dimensional radial averaged power spectrum

The 2D radial power spectrum technology gives a simple view of the depth distribution over the entire area. The district can be divided into two groups of residents; Deep and shallow. Each area's depth can be determined using the slope of each curve segment.

In this study, the energy spectrum is calculated using the Fast Fourier Transform (FFT) on the RTP magnetic data (Spector and Grant, 1970, Kivior and Boyd, 1998). Figure (9) depicts two distinct components as straight-line

segments, whose slopes are steeper as frequency and wavelength increase. By include the segment's slope in the formula, the depth of each source ensemble responsible for each segment was determined.

$$h=-s/4\pi \qquad (1)$$

Where ***h*** is the depth, ***s*** is the slope of the log power (energy) spectrum.

The energy spectrum is categorized into three parts.

a) The deeper source with wave number is (0.4)cycles/grid unit, and the depth is 1.546 km. as calculated from the eq. (6.1).
b) The Shallow source with a depth equal to 0.28315km as calculated from the previous equation, where the wave number is (1.4) cycles/grid unit.
c) Very shallow depth noise community and this indicates a small signal of high wave number from sources close to the surface.

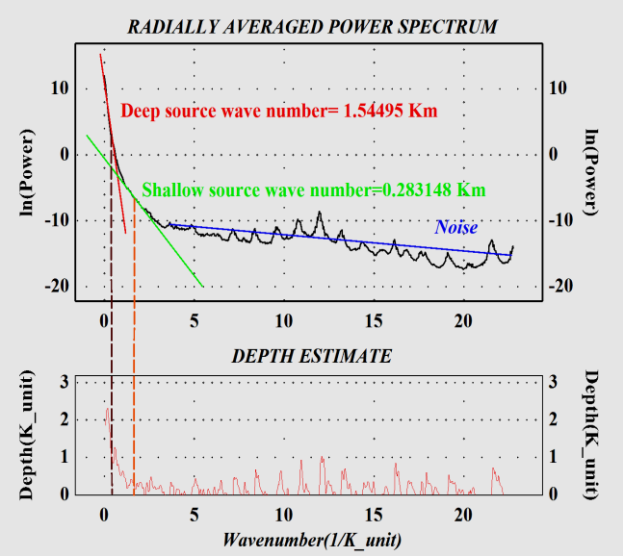

Fig.9. A 2D average power spectrum curve for the area under study.

3.3.2. Werner Method

Use the Werner Method (WERNER GX) in Geosoft Oasis Montaj to compute the Werner deconvolution solutions from magnetic profiles. This GX incorporates the iterative improvement plan outlined by Ku and Sharp (1983) and is based on the USGS program PDEPTH (Phillips, 1997). (1983). Four of the input channels, re-sampled to an even sample interval are copied to the output database: "Elev.", "Mag", "Horizontal Gradient", and "Topography". The "Elev" and "Topography" profiles are automatically plotted in the top pane; the "Mag" and "Horizontal Derivative" profiles are automatically plotted in the middle pane; also automatically plots the "Z dikes" and "Z Contacts" symbols in the bottom pane.

Eleven profiles (Fig.10) were used in this method, the output data examples are displayed in Figures (11 and 12) for illustration and Table (1). The average depth for the dykes in all profiles is (-36.3) m. and for the contacts is (-31.3) m.

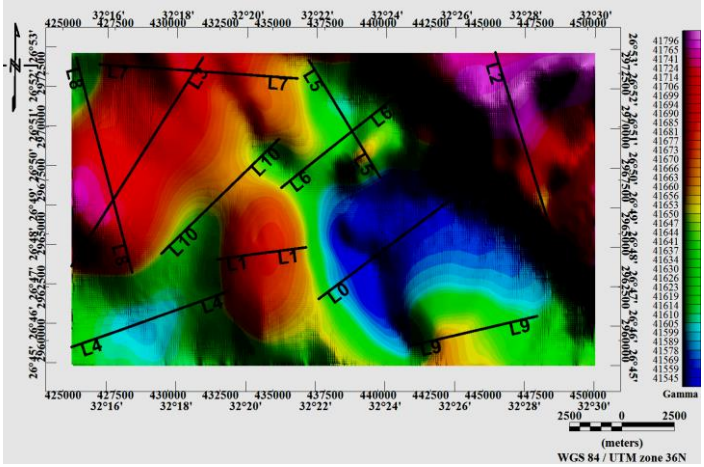

Fig.10. Location map of the selected profiles for the basement depth estimation from the RTP map using spectral analysis technique.

Table. 1. Values of the selected magnetic profiles' estimated basement depths as determined using Werner solutions.

Line No.	Depth (m) using Werner solutions					
	Dykes			Contacts		
	Max.	Min.	Aver.	Max.	Min.	Aver.
0	-4.7	-184.3	-37	-5.5	-133.1	-32.5
1	-6.7	-120.2	-38.4	-1	-101.6	-29.8
2	-5.9	-120	-38.1	-2.3	-125.3	-31.5
3	-6.6	-175.5	-37.4	-3.8	-207.4	-32.1
4	-4.9	-74.9	-29.7	-2.1	-205.3	-28.3
5	-5.6	-105.4	-41.1	-2.7	-107.6	-34.3
6	-8.2	-192.3	-43.1	-3	-209.7	-35.2
7	-3.8	-145.8	-30.2	-1.7	-106.7	-27.6
8	-4.3	-140.1	-35.2	-1.4	-85.6	-31.3
9	-2.7	-87.9	-31	-3.6	-102.8	-28.7
10	-6.1	-137.4	-38.1	-3.9	-114.2	-32.9

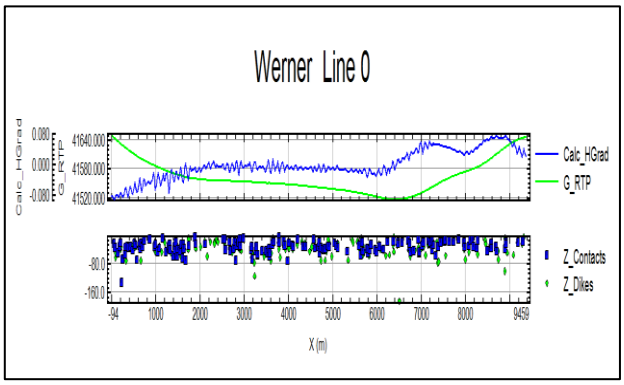

Fig.11 Estimated basement depth (dykes and contacts) values for the magnetic profile (0) using the Werner solutions technique.

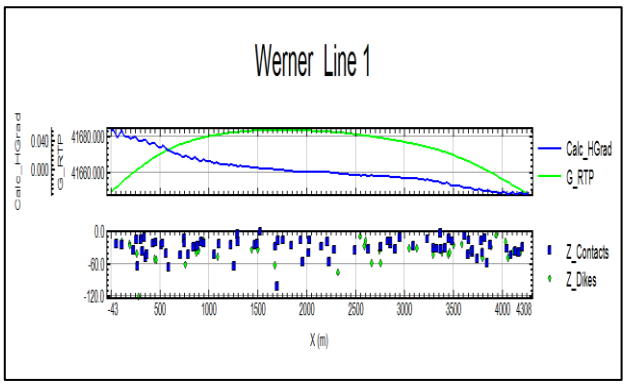

Fig. 12. Estimated basement depth (dykes and contacts) values for the magnetic profile (1) using the Werner solutions technique.

3.3.3. Euler deconvolution for the magnetic data

Using the Geosoft Oasis Montaj programme V.8.4 (2015), the Euler procedure was implemented to the RTP magnetic map of the area under investigation. Structural index (SI) equal to zero is used to calculate the Euler solutions in order to find magnetic connections (Durrheim and Cooper, 1998; Reid et al., 1990; and Thompson, 1982). To find the edges of thin sheets (sill, dike, etc.), use an Euler deconvolution with a structural index of one

The following represents brief description of the obtained Euler plots:

3.3.4. Euler map with Structural index equal to zero

The structural index with zero values, which is primarily used to identify the geological boundaries between major lithological units with various magnetic susceptibilities. The derived categorised Euler map (Fig.13) with a structural index of zero reveals the following:

1. The depth of the detected Euler anomalies is between 20 and 2000 meters. The maximum value is observed at scattered parts but it increases toward the western side of the mapped area.
2. Most of shallow contacts extend in the NE-SW direction, these lineaments increased in the southeast and the west directions.
3. The deepest trends are found in the western and northwestern regions of the research area, extending in the N-S and NE-SW directions, according to a thorough examination of the Euler anomaly clusters.
4. On the other hand, the Euler anomaly trends having shallower depth values are detected in the southern parts and on eastern parts of the study area. The location of these shallow Euler trends delimits the possibly boundaries of the uplifted basement blocks found in the study area.

Using structural index zero gives depth values more similar to those estimated by different depth estimation procedures that may be due to the magnetic contacts usually appear on surfaces of magnetic contrast, which related to lithology.

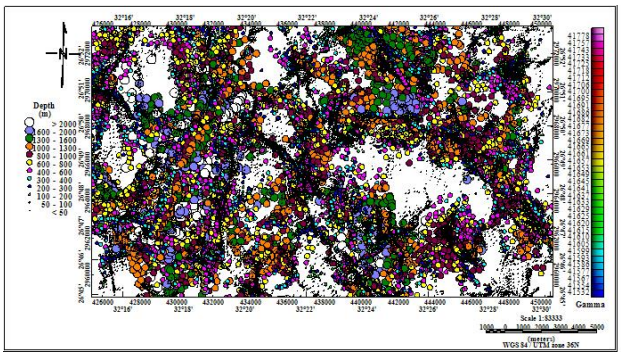

Fig. 13. Euler depth map with structural index equal to zero to find potential contacts' locations in the research region.

4. Conclusions

This study's goals are to assess the deformation resulting from the intrusion of igneous bodies within the sedimentary cover, Eastern Desert, Egypt. This affection caused deformation of the sedimentary cover. So, studying of the surface and the subsurface tectonic pattern which affected the basement relief and the overlying sedimentary cover is the main target in this study, in addition to estimation of the depth of the basement rock within the study region which indicates the thickness of the sedimentary cover. The underlying structures of the basement rock and the surrounding sedimentary cover were determined using magnetic dating and its derivatives by analysis of aeromagnetic data for the study region. The results demonstrate that the depth to the basement rock and the intrusions are ranging from 50 m to more than 1500 m in other areas away from the intrusions. surface structural analysis of fault trends from rose (azimuth frequency) diagrams indicated that the most predominant fault trends are N 40°- 55° E, N 60° –75° E, and N 30°-45° W trends, with less abundance of NNE-SSW and N-S. Most of the strata are dipping outward due to the injection of the tertiary basalt. The intrusion is forming in different phases where the dipping of the strata is varying from 40^{o} to 25^{o}. The

subsurface structural analysis indicated that the most dominant trend is the N-S. It was recorded more or less in all magnetic maps. It is referred to as the Nubian trend, was passed down through the basement rocks of Egypt, and is viewed as a continuation of the Mozambique belt. This trend is considered as a deformation strain resulting from a major stress affecting the study area in the direction perpendicular to this trend (E-W). The second trend is the NW–SE trend. It related to Eritrean and Gulf of Suez fault trend. It results due to NE-SW stress affecting the area. The third concluded trend is E-W (Tethyian trend). The majority of magnetic maps show this tendency. The most significant underlying trend, the E-W trend, appears on the surface map with very little extension. The majority of E-W lineaments are connections between basement rock units with various magnetic susceptibilities, which could be the cause. It is formed due to N-S stress affecting the study area. The fourth deduced trend is the NE – SW (Aqaba trend). This trend is the most significant surface structural trend in the examined area, although it is extremely uncommon as a subsurface structural trend. In Egypt's tectonic structure, it correlates to the Qattara trend.

5. References

1. Abdel Moneim A., (1988). Hydrogeology of the Nile basin in Sohag province. MSc Thesis, Geol. Dept., Fac. Sci., Assiut Univ., Egypt
2. Baranov, V., (1957). A New Method for Interpretation of Aeromagnetic Maps, Pseudo-Gravimetric Anomalies. Geophysics, 22, 359-363.
3. Blakely R.J., (1996). Potential theory in gravity and magnetic applications. Cambridge University Press,
4. Blakely R.J., Simpson R.W., (1986). Approximating edges of source bodies from magnetic or gravity anomalies Geophysics 51,1494-1498
5. Chennouf T., Khattach D., Milhi A., Andrieux P., Keating P. (2007). Principales lignes structurales du Maroc nord-oriental: apport de la gravimétrie Comptes Rendus Geoscience 339,383-395
6. Conoco, (1987). Geologic map of Egypt scale 1:500,000 Assiut and Bemi Suef, The Egyption General Petroleum Corporation (EGPC), Egypt
7. Cooper, G.R.J., (1997). GravMap and Pf Proc software for filtering geophysical map data. Comput. Geosci. 23 (1), 91–101.
8. Cordell L, Grauch, (1982). V Mapping Basement Magnetization Zones From Aeromagnetic Data In the San Juan Basin New Mexico. In: 1982 SEG Annual Meeting, Society of Exploration Geophysicists,
9. Cordell L., Grauch V. (1985). Mapping basement magnetization zones from aeromagnetic data in the The utility of regional gravity and magnetic anomaly maps:181
10. CONOCO (1987). Geological map of Egypt, Scale 1: 500,000, Assiut and Beni Suef. The Egyptian General Petroleum Corporation, Cairo (EGPC), Egypt.
11. Durrheim R.J., Cooper G.R.J., (1998). EULDEP: a program for the Euler deconvolution of magnetic and gravity data, Comput. Geosci. 24, 545–550.
12. EGPC and CONCCO (1987). Geological map of Egypt scale 1:500,000. Cairo, Egypt.
13. EGSMA (1983). Geological map of Gebel el “urf quadrangles, Egypt. scale 1:250000. Geological Survey Egypt. Cairo.
14. EGSMA (2006). Geological map of Abu had quadrangle. Egypt Scale 1:100000.
15. EGSMA (1983) Geological map of Gebel el ‘urf quadrangles, Egypt, scale 1:250000. Geological Survey Egypt, Cairo.
16. EGSMA (2006) Geological map of Abu had quadrangle. Egypt Scale 1:100000.
17. Everaerts M, Mansy J-L (2001). Le filtrage des anomalies gravimetriques; une cle pour la comprehension des structures tectoniques du Boulonnais et de l'Artois (France) Bulletin de la Société géologique de France 172,267-274
18. Gay S.P.Jr., (1972). Fundamental characteristics of aeromagnetic lineaments, their geologic significance, and their significant to geology. "The New Basement Tectonics" American Stereo Map Company, Salt Lake City, Utah:.94.
19. Hansen R., Pawlowski R. (1989). Reduction to the pole at low latitudes by Wiener filtering Geophysics 54,1607-1613
20. Hesham S.Z., Hesham T., (2016). Application of high-pass filtering techniques on gravity and magnetic data of the eastern Qattara Depression area, Western Desert, Egypt, NRIAG Journal of Astronomy and Geophysics, 5,106–123.
21. Ismaiel HA, Badry MM (2012). Geotechnical Evaluation of Sedimentary Rocks and Karstification Phenomena of Carbonates Exposed along New Upper Egypt-Red Sea Road, Eastern Desert, Egypt Journal of Earth Science and Engineering 2,636-647
22. Keheila EA, El-Ayyat AAM (1990). Lower Eocene carbonate facies, environments and sedimentary cycles in Upper Egypt: evidence for global sea-level changes Palaeogeography, Palaeoclimatology, Palaeoecology 81,33-47.
23. Khalil A., Abdel Hafeez T.H., Saleh H.S., Mohamed H. W., (2016). Inferring the subsurface basement depth and the structural trends as deduced from aeromagnetic data at West Beni Suef area, Western Desert, Egypt, NRIAG Journal of Astronomy and Geophysics, 5, 380–392.
24. Khattach D, Mraoui H, Sbibih D, Chennouf T (2006). Analyse multi-échelle par ondelettes des contacts géologiques: application à la carte gravimétrique du Maroc nord-oriental Comptes Rendus Geoscience 338,521-526
25. Kivior I., Boyd D., (1998). Interpretation of the

aeromagnetic experimental survey in the Eromanga/Cooper basin. Can. J. Explor. Geoph., 34, 58-66.
26. Ku, C.C. and Sharp, J.A., (1983). Werner deconvolution for automated magnetic interpretation and its refinement using Marquart's inverse modeling. Geophysics, 48(6),754-774
27. Phillips, J. D., (1997). Potential-Field Geophysical Software for the PC, version 2.2: USGS Open-File Report 97-725.
28. Reid A.B., Allsop J.M., Granser H., Millett A.J. and Somerton I.W., (1990). Magnetic interpretation in three dimensions using Euler Deconvolution. Geophysics, 55, 80-90.
29. Shaaban MN (2004). Diagenesis of the lower Eocene Thebes Formation, Gebel Rewagen area, Eastern Desert, Egypt Sedimentary Geology 165.53-65
30. Spector, A. and Grant, F.S. (1970). Statistical models for interpreting aeromagnetic data. Geophysics, Vol. 35, PP. 293-302.
31. Thompson D.T., (1982). EULDPH- A New technique for making computer-assisted depth estimates from magnetic data. Geophysics, 47.31–37.